Original Research Paper

Volume-8 | Issue-3 | March-2018 | PRINT ISSN No 2249-555X

Engineering

# SIMULATION AND IMPLEMENTATION OF SOLAR POWER OPTIMIZER FOR DC DISTRIBUTION SYSTEM

**Nimain Charan Nayak** Associate Professor, Department of Electrical and Electronics Engineering MNM Jain Engineering College, Chennai, India

**ABSTRACT** This paper presents "Simulation and Implementation of Solar Power Optimizer for DC Distribution System". A high step-up solar power optimizer (SPO) that efficiently harvests maximum energy from a photovoltaic (PV) panel then outputs energy to a dc-micro grid. Its structure integrates coupled inductor and switched capacitor technologies to realize high step-up voltage gain. The leakage inductance energy of the coupled inductor can be recycled to reduce voltage stress and power losses. A low voltage rating and low-conduction resistance switch improves system efficiency by employing the incremental conductance method for the maximum power point tracking (MPPT) algorithm. Because of its high tracking accuracy, the method is widely used in the energy harvesting of PV systems. The power reduction that is caused by the shadow effect is an inevitable problem in a centralized PV system. The use of a micro inverter or ac module has recently been proposed for individual PV panels.

**KEYWORDS :** High Step-Up Voltage Gain, Maximum Power Point Tracking (MPPT), Solar Power Optimizer (SPO).

## I. INTRODUCTION

The paper titled "Simulation and Implementation of Solar Power Optimizer for DC Distribution System" a development of in the cited papers, A photovoltaic (PV) power generation system, which uses a renewable resource, has been extensively used in emergency facilities and in generating electricity for mass use. A conventional PV generation system is either a single- or a multi string PV array that is connected to one or several central PV inverters. Numerous series-connected PV modules are connected in the PV array to achieve the DC link voltage that is high enough to be connected to electricity through the DCAC inverter. However, the power reduction that is caused by the shadow effect is an inevitable problem in a centralized PV system. The use of a micro inverter or ac module has recently been proposed for individual PV panels. Although this discrete PV power generation solution may partially eliminate the shadow problem, a micro inverter structure constrains the system energy's harvesting efficiency and entails high costs. The SPO attempts to improve the use of distributed renewable resources and lower system cost. It may also potentially improve the efficiency of PV systems, has an anti-shadow effect, and can monitor the status of PV modules. Moreover, the dc-grid voltage is regulated by bidirectional inverter and battery tank. In case of low-loading condition, the redundant energy will store into battery or through bidirectional inverter to ac grid. A solar power optimizer (SPO) was developed as an alternative to maximize energy harvest from each individual PV module.

The objective of this paper is one of the most high step-up solar power optimizer (SPO) that efficiently harvests maximum energy from a photovoltaic (PV) panel then outputs energy to a dc-micro grid. Its structure integrates coupled inductor and switched capacitor technologies to realize high step-up voltage gain. The leakage inductance energy of the coupled inductor can be recycled to reduce voltage stress and power losses. A low voltage rating and low-conduction resistance switch improves system efficiency by employing the incremental conductance method for the maximum power point tracking (MPPT) algorithm. Because of its high tracking accuracy, the method is widely used in the energy harvesting of PV systems. A photovoltaic (PV) power generation system, which uses a renewable resource, has been extensively used in emergency facilities and in generating electricity for mass use. A conventional PV generation system is either a single- or a multi string PV array that is connected to one or several central PV inverters. Numerous series-connected PV modules are connected in the PV array to achieve the DC link voltage that is high enough to be connected to electricity through the DC and AC inverter.

## II. PROPOSED SYSTEM

Fossil fuels continue to be depleted, and their use has been instrumental to climate change, a problem that grows more severe each year. A photovoltaic (PV) power generation system, which uses a renewable resource, has been extensively used in emergency facilities and in generating electricity for mass use. A conventional PV generation system is either a single- or a multi string PV array that is connected to one or several central PV inverters. Numerous series-connected PV modules are connected in the PV array to achieve the DC link voltage that is high enough to be connected to electricity through the DCAC inverter. However, the power reduction that is caused by the shadow effect is an inevitable problem in a centralized PV system. The use of a micro inverter or ac module has recently been proposed for individual PV panels. Although this discrete PV power generation solution may partially eliminate the shadow problem, a micro inverter structure constrains the system energy's harvesting efficiency and entails high costs.

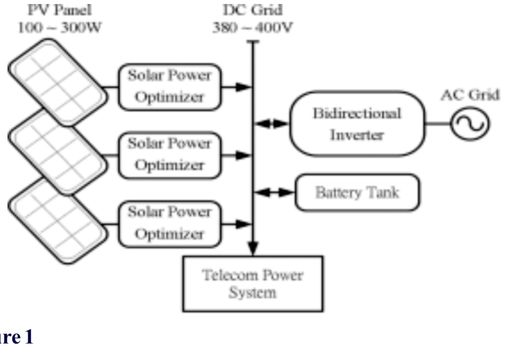


**Figure 1**

A solar power optimizer (SPO) was developed as an alternative to maximize energy harvest from each individual PV module. An SPO is used as a dc–dc converter with maximum power point tracking (MPPT), which increases PV panel voltage to optimum voltage levels for a dc microgram connection or through a dc–ac inverter for electricity [3]–[6]. Fig. 1 shows a single PV panel's energy, which passes through an SPO to a dc microgrid system. A 400 V dc-microgrid system was proposed as an energy-efficient distribution option for data centre systems and telecommunication facilities. The SPO attempts to improve the use of distributed renewable resources and lower system cost. It may also potentially improve the efficiency of PV systems, has an anti shadow effect, and can monitor the status of PV modules. Moreover, the dc-grid voltage is regulated by bidirectional inverter and battery tank. In case of low-loading condition, the redundant energy will store into battery or through bidirectional inverter to ac grid.

The maximum power point (MPP) voltage range of a single PV panel ranges from 15 to 40 V and has a power capacity of about 100 to 300 W [9]. An SPO has a high step-up converter that increases low-input voltage to a sufficient voltage level. Various step-up dc–dc converter topologies include a conventional boost and flyback converters, switched inductor converter, and switched capacitor converter, as well as a transformer less switched capacitor types, voltage lift types, capacitor–diode voltage multipliers, and boost types that are integrated with coupled inductors. With increasing voltage gain, recycling the leakage inductance energy of a coupled inductor will reduce the voltage stress on the active switch, which enables the coupled Inductor and voltage multiplier or voltage-lift technique to realize high-voltage gain

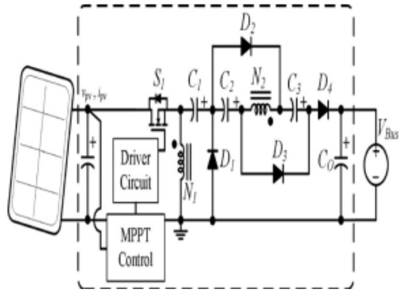


**Figure 2**

high step-up dc–dc converter with an MPPT control circuit. The converter includes a floating active switch S and a coupled inductor T1 with primary winding N1, which is similar to the input inductor of a conventional boost converter capacitor C1, and diode D1 recycle leakage inductance energy from N1. Secondary winding N2 is connected to another pair of capacitors, C2 and C3, and to diodes D2 and D3. Rectifier diode D4 connects to output capacitor Co and load R. The duty ratio is modulated by the MPPT algorithm, which uses the incremental conductance method that is employed in the proposed SPO. It detects PV module voltage Vpv and current Ipv to determine the increase and decrease in the duty cycle of the dc converter. Therefore, the MPP can be obtained by comparing instantaneous conductance I/V and incremental conductance dI/dV. The algorithm is programmed into TMS320LF2407A, a digital signal microprocessor. The proposed converter has the following features: 1) its voltage conversion ratio is efficiently increased by using the switched capacitor and coupled inductor techniques; 2) the leakage inductance energy of the coupled inductor can be recycled to increase efficiency, and the voltage spike on the active switch is restrained; 3) the floating active switch isolates the PV panel's energy during non operating conditions, thereby preventing any potential electric hazard to humans or facilities. The MPPT control algorithm exhibits high-tracking efficiency; hence, it is widely used in the energy harvesting of PV systems. The rest of the paper is organized as follows. Sections II and III discuss the operating principle and steady-state analysis of the proposed converter, respectively. Section IV addresses the practical implementation and component selection of the proposed converter. Section V presents the experimental results, and VI concludes the paper.

## III. OPERATING PRINCIPLE

The operating principles for continuous conduction mode (CCM) and discontinuous conduction mode (DCM) are presented in detail. Fig. 3 illustrates a typical waveform of several major components in CCM operation during one switching period. To simplify the circuit analysis of the proposed converter, the following assumptions are made:

1) All components are ideal, except for the leakage inductance of coupled inductor T1, which is taken into account. On-state resistance RDS (ON) and all the parasitic capacitances of main switch S are disregarded, as are the forward voltage drops of diodes D1 to D4 ;
2) Capacitors C1 to C3 and Co are sufficiently large that the voltages across them are considered constant;
3) The equivalent series resistance (ESR) of capacitors C1 to C3 and Co, as well as the parasitic resistance of coupled inductor T1, is neglected;
4) Turns ratio n of coupled inductor T1 windings is equal to N2 /N1. The CCM operating modes are described as follows.

*CCM Operation*

*Mode I* **[t0, t1]:** During this interval, switch S and diodes D2 and D3 are conducted; diodes D1 and D4 are turned OFF. The current flow path is shown in Magnetizing inductor Lm continues to release energy to capacitors C2 and C3 through secondary winding N2 of coupled inductor T1. Leakage inductance Lk 1 denotes the stored energy from source energy Vin. The energy that is stored in capacitor Co is constantly discharged to load R. This mode ends when increasing iLk1 is

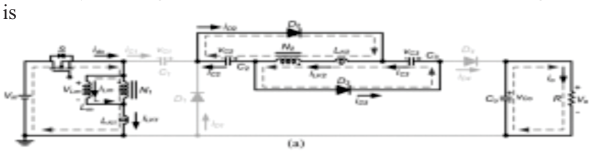

(a)

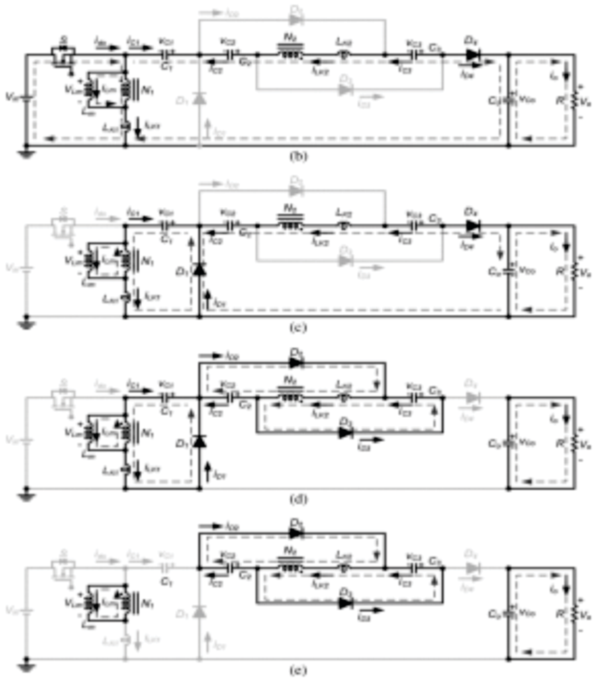

(b) (c) (d) (e)

CCM operation: (a) Mode I, (b) Mode II, (c) Mode III, (d) Mode IV, and (e) Mode V.

Equal to decreasing iLm at t = t1

$$v_{Lm} = V_{\text{in}}$$

$$\Delta i_{Lm} = \frac{V_{\text{in}}}{L_m}(t_1 - t_0).$$

*Mode II* **[t1, t2]:** During this interval, switch S and diode D4 are conducted. Source energy Vin is serially connected to C1, C2, and C3, and secondary winding N2; Lk2 discharges the energy that is stored in charge output capacitor Co and loads R. Meanwhile, magnetizing inductor Lm also receives energy from Vin. The current flow path is shown in Fig. 4(b). This mode ends when switch S is turned OFF at t = t2

$$v_{Lm} = \frac{V_o - V_{\text{in}} - V_{c1} - V_{c2} - V_{c3}}{n}$$

$$n = \frac{N_2}{N_1}$$

$$\Delta i_{Lm} = \frac{V_o - V_{\text{in}} - V_{c1} - V_{c2} - V_{c3}}{n \cdot L_m} \cdot (t_2 - t_1).$$

*Mode III* **[t2, t3]:** During this transition interval, switch S and diodes D2 and D3 are turned OFF, and diodes D1 and D4 are conducted. The current flow path is shown in Fig. 4(c). The energy stored in leakage inductance Lk 1 instantly flows through the diode D1 to charge capacitor C1. The energy is released to magnetizing inductor Lm through coupled inductor T1, which is serially connected to C1, C2, and C3, and secondary winding N2; Lk2 discharges the energy that is stored in charge output capacitor Co and loads R. This mode ends when decreasing iLk1 is equal to increasing iLm at t = t3

$$v_{Lm} = -V_{c1}$$

$$\Delta i_{Lm} = \frac{-V_{c1}}{L_m} \cdot (t_3 - t_2).$$

*Mode IV* **[t3, t4]:** During this interval, switch S and diode D4 are turned OFF, and diodes D1, D2, and D3 are conducted. The current flow path is shown in Fig. 4(d). Leakage inductance Lk 1 continues to release energy to charge capacitor C1 through diode D1. Magnetizing inductor Lm through coupled inductor T1 transfers energy to capacitors C2 and C3. The energy that is stored in capacitor CO is constantly discharged to load R. This mode ends when decreasing iLk1 is zero at t = t4

$$v_{Lm} = -V_{c1}$$

$$\Delta i_{Lm} = \frac{-V_{c1}}{L_m} \cdot (t_4 - t_3).$$

*Mode V* **[t4, t5]:** During this interval, diodes D2 and D3 are conducted. The current flow path is shown in Fig. 4(e). Magnetizing inductor Lm constantly transfers energy to secondary winding N2, and charges capacitors C2 and C3. The energy that is stored in capacitor CO is constantly discharged to load R. This mode ends when switch S is turned ON at the beginning of the next switching period

$$v_{Lm} = \frac{-V_{c2}}{n} = \frac{-V_{c3}}{n}$$

$$\Delta i_{Lm} = \frac{-V_{c2}}{n \cdot L_m} \cdot (t_5 - t_4) = \frac{-V_{c3}}{n \cdot L_m} \cdot (t_5 - t_4).$$

*DCM Operation*

*Mode I* **[t0, t1]:** During this interval, switch S and D4 are conducted, and diodes D1, D2, and D3 are turned OFF. The current flow path is shown in Fig. 6(a).Magnetizing inductor Lm with leakage inductance Lk 1 stores energy from source energy Vin. Meanwhile, source energy Vin is also serially connected to capacitors C1, C2, and C3, and secondary winding N2 to charge capacitor Co and load R. This mode ends when switch S is turned OFF at t = t1

$$v_{Lm} = V_{in} = \frac{V_o - V_{in} - V_{c1} - V_{c2} - V_{c3}}{n}$$

$$\Delta i_{Lm} = \frac{V_{in}}{L_m} \cdot (t_1 - t_0) = \frac{V_o - V_{in} - V_{c1} - V_{c2} - V_{c3}}{n \cdot L_m} \cdot (t_1 - t_0).$$

*Mode II* **[t1, t2]:** During this transition interval, switch S and diodes D2 and D3 are turned OFF, and diodes D1 and D4 are conducted. The current flow path is shown in Fig. 6(b). The energy stored in leakage inductance Lk 1 instantly flows through the diodeD1 to charge capacitor C1; this energy is also released to magnetizing inductor Lm through the coupled inductor T1 series that is connected to C1, C2, and C3, secondary winding N2, and Lk2 to charge output capacitor Co and load R. This mode ends when decreasing iD4 is zero at t = t2

$$v_{Lm} = -V_{c1}$$

$$\Delta i_{Lm} = \frac{-V_{c1}}{n \cdot L_m} \cdot (t_2 - t_1).$$

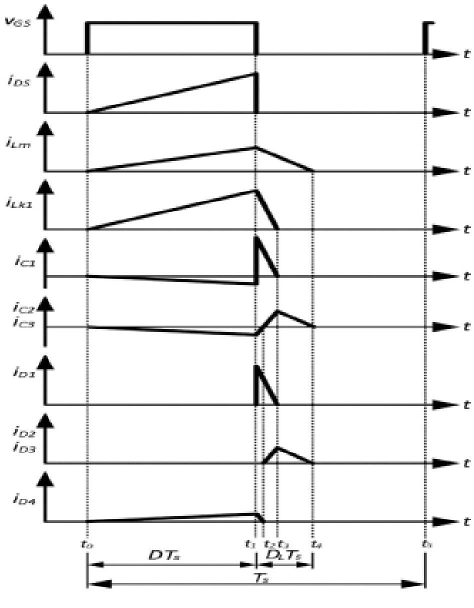


*Mode III* **[t2, t3]:** During this transition interval, switch S and diode D4 are turned OFF, and diodes D1, D2, and D3 are conducted. The current flow path is shown in Fig. 6(c). Leakage inductance Lk 1 continues to release energy to charge capacitor C1 through diode D1. Magnetizing inductor Lm transfers energy to capacitors C2 and C3 through coupled inductor T1. The energy stored in capacitor Co is constantly discharged to load R. This mode ends when decreasing iLk1 is zero at t = t3

$$v_{Lm} = -V_{c1} = \frac{-V_{c2}}{n} = \frac{-V_{c3}}{n}$$

$$\Delta i_{Lm} = \frac{-V_{c1}}{n \cdot L_m} \cdot (t_3 - t_2) = \frac{-V_{c2}}{n \cdot L_m} \cdot (t_3 - t_2) = \frac{-V_{c3}}{n \cdot L_m} \cdot (t_3 - t_2).$$

*Mode IV* **[t3, t4]:** During this interval, switch S, diodes D1 and D4 are turned OFF, and diodes D2 and D3 are conducted. The current flow path is shown in Fig. 6(d).Magnetizing inductor Lm constantly transfers energy to secondary winding N2 and charges capacitors C2 and C3. The energy that is stored in capacitor Co is constantly discharged to load R. This mode ends when decreasing iLm is zero at t = t4

$$v_{Lm} = \frac{-V_{c2}}{n} = \frac{-V_{c3}}{n}$$

$$\Delta i_{Lm} = \frac{-V_{c2}}{n \cdot L_m} \cdot (t_5 - t_4) = \frac{-V_{c3}}{n \cdot L_m} \cdot (t_4 - t_3).$$

*Mode V* **[t4, t5]:** During this interval, the switch and all the diodes are turned OFF. The current flow path is shown in Fig. 6(e). The energy that is stored in capacitor CO is constantly discharged to load R. This mode ends when switch S is turned ON at the beginning of the next switching period

$$v_{Lm} = 0$$

$$\Delta i_{Lm} = 0.$$

## IV. SIMULATION RESULT

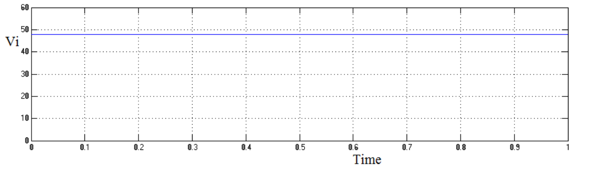


(a).DC input current

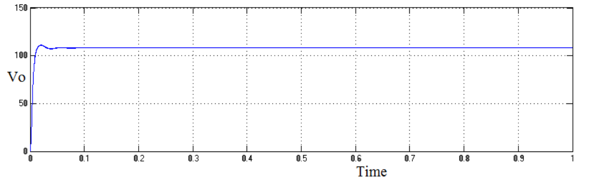


(b).DC output voltage

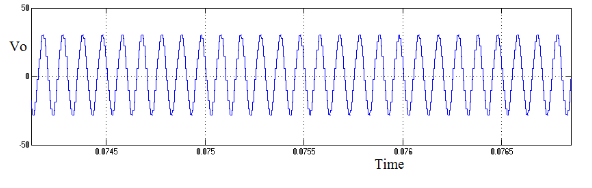


(c).AC output voltage

## V. CONCLUSION

The high step-up SPO uses the coupled inductor with an appropriate turn's ratio design and switched-capacitor technology to achieve a high-voltage gain that is 20 times higher than the input voltage. Because the leakage inductance energy of a coupled inductor is recycled and the voltage stress across the active switch S is constrained, the low RDS (ON) of active switch can be selected to improve maximum efficiency up to 96.7%. As a result, full load efficiency reaches 92.8%. The highest MPPT accuracy is 99.9% and the highest average accuracy is 97.9% at PPV = 150 W. A 300 W SPO with a high step-up voltage gains and MPPT functions are implemented and verified.

The basic circuit and modified circuit elements are designed using relevant equations. The simulation circuits are developed using elements of simulink library. The Simulation is successfully done and open loop / closed loop simulation results are presented. The Simulation results coincide with the theoretical results.

## REFERENCE


[1] Y. Fang and X. Ma, "A novel PVmicroinverter with coupled inductors and double-boost topology," IEEE Trans. Power Electron., vol. 25, no. 12, pp. 3139–3147, Dec. 2010.

[2] A. Ch. Kyritsis, E. C. Tatakis, and N. P. Papanikolaou, "Optimum design of the current-source fly back inverter for decentralized grid-connected photovoltaic systems," IEEE Trans. Energy Convers., vol. 23, no. 1, pp. 281–293, Mar. 2008.

[3] P. Tsao, "Simulation of PV systems with power optimizers and distributed power electronics," in Proc. IEEE Photo volt. Spec. Conf., Jun. 2010, pp. 389–393.

[4] D. D.-C. Lu and V. G. Agelidis, "Photovoltaic-battery-powered DC bus system for common portable electronic devices," IEEE Trans. Power Electron., vol. 24, no. 3, pp. 849–855, Feb. 2009.

[5] L. Zhang, K. Sun,Y. Xing, L. Feng, andH.Ge, “A modular grid-connected photovoltaic generation system based on DC bus,” IEEE Trans. Power Electron., vol. 26, no. 2, pp. 523–531, Feb. 2011.
[6] S. M. Chen, K. R. Hu, T. J. Liang, L. S. Yang, and Y. H. Hsieh, “Implementation of high step-up solar power optimizer for DC micro grid application,” in Proc. IEEE Appl. Power Electron Conf., Feb. 2012, pp. 28–32.
[7] A. Pratt, P. Kumar, and T. V. Aldridge, “Evaluation of 400 V DC distribution in telco and data centers to improve energy efficiency,” in Proc. IEEE Int. Telecommun. Energy Conf., Sep./Oct. 2007, pp. 32–39.
[8] L. Zhang, K. Sun,Y. Xing, L. Feng, and H.Ge, “A modular grid-connected photovoltaic generation system based on DC bus,” IEEE Trans. Power Electron., vol. 26, no. 2, pp. 523–531, Feb. 2011.
[9] S.M. Chen, T. J. Liang, L. S. Yang, and J. F. Chen, “A boost converter with capacitor multiplier and coupled inductor for AC module applications,” IEEE Trans. Ind. Electron., Early Access Articles, vol. PP, no. 99, p. 1.
[10] A. C. Nanakos, E. C. Tatakis, and N. P. Papanikolaou, “A weighted efficiency- oriented design methodology of fly back inverter for AC photovoltaic modules,” IEEE Trans. Power Electron., vol. 27, no. 7, pp. 3221–3233, Jul. 2012.